Chapter 9
Electrochemical Techniques for the Study of Self Healing Coatings

Y. Gonzalez-Garcia, S.J. Garcia and J.M.C. Mol

9.1 Electrochemistry in the Context of Corrosion

As discussed in chapter one, corrosion can be defined as the degradation of the material properties due to its interaction with the environment [1]. In general this interaction takes place by an electrochemical reaction. While in chemical reactions elements are added or removed from a chemical species in electrochemical reactions electrons are also involved in the process. In electrochemical reactions elements might be added or removed from a chemical species but also at least one species undergoes a change in the number of valence electrons (oxidation or reduction). Electrochemistry is thus the branch of chemistry focused mainly on the study of chemical changes caused by the passage of an electric current and the production of electrical energy by chemical reactions.

There are four necessary prerequisites for electrochemical reactions to take place thereby triggering the corrosion process: an anode (where oxidation occurs), a cathode (where reduction takes place consuming the electrons released from the anode), an electrolytic path for ionic conduction between the two reaction sites, and an electrical path for electron conduction between the reaction sites. These requirements are illustrated schematically in Fig. 9.1.

Y. Gonzalez-Garcia (✉) · J.M.C. Mol
Materials Science & Engineering Department, Delft University of Technology,
Mekelweg 2 2628 CD, Delft, The Netherlands
e-mail: y.gonzalezgarcia@tudelft.nl

S.J. Garcia
Novel Aerospace Materials, Delft University of Technology,
Kluyverweg 1 2629 HS, Delft, The Netherlands

A.E. Hughes et al. (eds.), *Active Protective Coatings*,
Springer Series in Materials Science 233, DOI 10.1007/978-94-017-7540-3_9

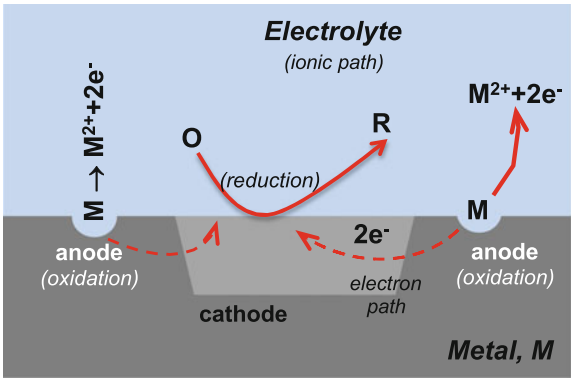

Fig. 9.1 Diagram displaying the main elements required for a corrosion process to occur: anode, cathode, electron path and ionic path

Corrosion research requires a thorough understanding of the electrochemical events within a particular metal-electrolyte system. The driving force for electrochemical events must be known in order to classify the type of electrochemical cell to be characterized to prevent corrosion.

9.2 Electrochemical Evaluation of Self-healing/Self-repair Coatings

In most metal applications, coatings are required to prevent the systems from fast corrosion or degradation. The underlying protection of coatings relies on barrier, adhesion, and active protection. The active protection mechanism is being improved using active and responsive materials (i.e. "smart coatings"). Such systems provide on-demand resistance to corrosion upon mechanical or chemical damage [1]. Such coatings inhibit corrosion processes of the underlying metal by active release of inhibiting species or by the on-demand or autonomous closure/repair of the damage. Significant research effort has focused on finding alternatives to introduce corrosion inhibitors into the organic coating. The traditional approach of using inhibitors is by their direct mixing with the coating binder, however problems such as dispersion and interaction with the polymer matrix affecting the release kinetics and inhibiting efficiency are likely to occur. In order to avoid such interactions encapsulation strategies of the corrosion inhibitor or healing agent have been proposed [2, 3] (see also Chap. 8). The incorporation of corrosion inhibitors into capsules is intended for controlled and effective release of the inhibitor. Therefore, an ideal performance of these encapsulated systems, would release the inhibiting species only when they are needed. The triggering of the inhibitor release can be established according to different mechanisms: breakdown

by mechanical damage, pH, dissolution, exchange, humidity or moisture, to name a few. In the end, the ability to suppress or decrease corrosion to tolerable levels will depend on efficiency of the healing behavior of the coating system. It is at this point where the evaluation methods are relevant. The techniques used for evaluation of (self-healing) anticorrosive coatings can be divided in three main groups:

- accelerated tests used in industry
- conventional (global) electrochemical methods, and
- localized electrochemical techniques.

Accelerated testing is possibly the most widespread methodology for corrosion resistance evaluation at an industrial scale and presents many different variants and adaptations. These tests are typically based on exposure of the material to controlled (atmospheric) severe conditions: humidity, salinity, pollutants, temperature, etc. Alternating wet/dry cycles changes the thickness of electrolyte layer. The presence of water, temperature, and chloride ions promotes the corrosion processes at the scribe (degree of corrosion) as well as at the intact coating (delamination, blisters). The degradation of coated metals (or materials in general) is assessed by visual inspection. Accelerated tests only provide information that allows a ranking of the specimen from "unacceptable" to "excellent". They are screening methods to differentiate corrosion performance of the specimen under study. However, accelerated test results form no basis for the understanding of the corrosion (or protection) mechanism. These types of evaluation can accumulate sometimes large amounts of error due to the extreme aggressive conditions, the long duration of the test and a subjective, user-dependent evaluation. Moreover, despite all its drawbacks, since it is used broadly in industry, this is an almost mandatory technique before any system is introduced in the market. More about the evaluation and application of self-healing systems from an industrial point of view is discussed in Chaps. 12–14.

To gain insight into the healing-process behind the behaviour of the system other techniques have to be used. These techniques include electrochemical techniques described in this chapter and physico-chemical characterization described in Chap. 10.

Electrochemical methods are versatile and they can provide a wide range of information that can include the understanding of multi-step reactions, the kinetics of heterogeneous electron-transfer reactions, coupled chemical reactions and adsorption processes. For corrosion studies, electrochemical evaluation provides valuable information such as kinetics of the corrosion or protection processes, formation of protective films, evolution of barrier properties, identification and quantification of redox species.

Potential measurements, potentiodynamic experiments (including polarization curves and cyclic voltammetry) and electrochemical impedance spectroscopy (EIS) are the most common electrochemical methods used for corrosion and self-healing research. In this chapter they are classified as global methods. More

advanced techniques that provide electrochemical properties with spatial resolution are considered localized techniques. Within this group micro-capillary cell, scanning vibrating electrode technique (SVET) and scanning electrochemical microscope (SECM) are included.

It is very important to identify the information that we can obtain from the electrochemical evaluation as function of the self-healing system under investigation. A summary of the information to be retrieved from electrochemical evaluation is presented in the Table 9.1. Three main types of healing-mechanism are considered: active and physical healing.

Table 9.1 Summary of the electrochemical techniques used to evaluate self-healing processes

Type of healing	System	Information	Electrochemical technique
Active	Corrosion inhibitor in solution	Screening of inhibitors	Potentiodynamic measurements
			High-throughput (multi-electrode) approach
		Mechanistic information	Electrochemical Impedance Spectroscopy (EIS)
		Kinetics of protection mechanism	
		Protection efficiency	Localized information: SVET
		Inhibition mechanism (localized)	Electrochemical microcapillary cell
Active-smart release	Inhibitor or healing agent incorporated into coating (directly in matrix or with micro-carriers)	Barrier properties of the coating	Electrochemical Impedance Spectroscopy (EIS)
		Kinetics of healing process (release)	
		Efficiency of the healing (protection) for long immersion time	
		Efficiency of healing (localized in the defect) for short immersion time	Scanning Vibrating Electrode Technique (SVET)
			Scanning Electrochemical Microscope (SECM)
		Properties of the coating around defect and healing activity in the defect	Local Electrochemical Impedance Spectroscopy (LEIS)

(continued)

Table 9.1 (continued)

Type of healing	System	Information	Electrochemical technique
Active-physical recovery	Smart polymeric coatings	Healing of barrier properties of the coating	Electrochemical Impedance Spectroscopy (EIS)
		Fast and quantitative information about the healing degree	AC/DC/AC technique
		Localized evaluation of the defective zone after healing process	Local Electrochemical Impedance Spectroscopy (LEIS)
		Confirmation of hindered corrosion activity after (localized) defect healing	Scanning Vibrating Electrode Technique (SVET)
			Scanning Electrochemical Microscope (SECM)

9.3 Conventional Electrochemical Techniques

In conventional electrochemical experiments, the electrode (metal) response to a perturbation signal corresponds to a surface-averaged measurement attributable to the behaviour of the whole electrode surface.

9.3.1 Open Circuit Potential

Measurements of the open circuit potential (OCP) as function of time is commonly used to study healing recovery of corroding metals.

When using this technique complementary tests are recommended to confirm the healing efficiency nevertheless it can be used as a first order approximation technique.

9.3.2 Potentiodynamic Measurements

Potentiodynamic methods consist of forcing the electrode potential to follow a known potential scan. The potential may be held constant or may be varied with time in a predetermined manner as the current is measured as a function of time or potential. In general, for these methods, systems in which the mass transport of electroactive species occurs only by diffusion should be considered.

Linear sweep voltammetry, alternatively named polarization curve measurement, is the most common potentiodynamic measurement. In Fig. 9.2 a scheme of polarization curve for a metal M during immersion in aqueous solution.

From polarization curves, the corrosion current density (i_{corr}) can be extrapolated from the linear parts of the Tafel plots (blue lines in Fig. 9.2). The intersection of the lines for cathodic and anodic processes correspond to the values of the corrosion current density. The linear parts of the curves should be in the range of potential ±150 mV above the corrosion potential (E_{corr}) value.

Another alternative to obtain the corrosion current is the linear polarization resistance (LPR) method. The polarization resistance of a material is defined as the slope of the potential-current density ($\Delta E/\Delta i$) curve at the free corrosion potential. Resistance polarization refers to the potential drop due to either the high resistivity of the electrolyte surrounding the electrode or an insulation effect of the film on the electrode surface formed by the reaction products.

Polarization resistance R_p is related to the corrosion current by the Stern-Geary equation:

$$R_p = \frac{B}{i_{corr}} = \frac{(\Delta E)}{(\Delta i)}_{\Delta E \to 0} \tag{9.1}$$

where, ΔE is a variation of the applied potential around the corrosion potential and Δi is the resulting polarization current. The proportionality constant, B, for a particular system can he determined empirically (calibrated from separate weight loss measurements) or, as shown by Stern and Geary, can be calculated from b_a and b_c, the slopes of the anodic and cathodic Tafel slopes:

$$B = \frac{b_a b_c}{2.3(b_a + b_c)} \tag{9.2}$$

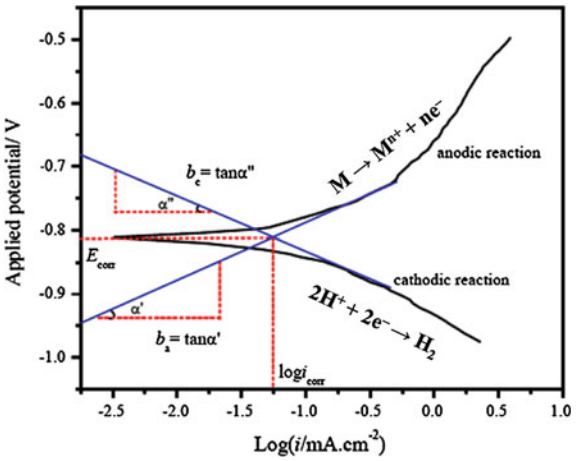

Fig. 9.2 Example of polarization *curve* for a metal M in an acidic environment. E_{corr} and i_{corr} are estimated by the intersection of the linear section of the *curves* corresponding to the Tafel *slope*

The Tafel slopes themselves can be evaluated experimentally using real polarization plots. A high R_p for a metal implies high corrosion resistance and a low R_p implies low corrosion resistance.

The extrapolation from the Tafel curves is only valid when the anodic and cathodic reactions are under activation control. In practice, determining the linear section of the Tafel plot is not always straightforward. Experimental polarization curves sometimes can present peculiarities that bring doubts about where to choose the linear section in the curve. This issue is a regular cause of errors when estimating the corrosion current.

Corrosion current is correlated to corrosion rate (r) of the process through Faraday's law by the following equation:

$$r = \frac{ai_{corr}}{nFD} \tag{9.3}$$

where a is the atomic number of the metal, n number of electrons, F the Faraday constant and D the density of the metal.

Within the context of self-healing materials, polarization methods are commonly used to evaluate and compare corrosion inhibitor performance in solution. The test consists of analyzing the response of the metal while it is immersed in solution containing dissolved corrosion inhibitor [4]. The resulting polarization curves give access to the corrosion rate. Furthermore it visualizes the anodic, cathodic or mixed protection performance of the inhibitor (Fig. 9.2). The analysis of the curves and interpretation of the results is well explained in Chap. 4.

Conventional potentiodynamic methods are usually not applicable for coated substrates due to important limitations arising from the high IR drop over the coating. This method cannot give any useful information on the active corrosion protection and the self-healing ability of protective coatings.

An alternative is the direct current (DC) measurement. For this case the coated sample is kept at high constant potential (potentiostatic method) and the current that flows through the system is measured. The electrochemical measurements are carried out in an electrochemical cell with typically a three electrode system (working, reference and counter electrodes) immersed in an electrolyte. The application of this constant potential can fully reduce or oxidize species in a given solution depending on the potential values, the substrate, pH of the electrolyte and other factors. It moves the systems out of electrochemical equilibrium possibly leading to (i) accelerated degradation of the system; or (ii) forced deposition-reaction of healing agents.

This technique has been used to study the healing capabilities of epoxy-amine coating doped with organic fillers containing inorganic corrosion inhibitors on steel [1] by monitoring the current density values at fixed potential (-0.85 $V_{Ag/AgCl}$ and -1.1 $V_{Ag/AgCl}$) with time. In this study, healing was detected by a decrease of the current density in a scratched doped-system, while the non-doped one showed an increase. The same system evaluated by electrochemical impedance spectroscopy (EIS) only showed a slight improvement with respect to the reference one. A similar

method has been also employed to assess healing of a steel plate coated with a self-healing coating using microencapsulation of liquid healing agents [5]. In this case, the experiment was performed at 3 V polarization measuring the current density evolution with time of the scratched samples. Healed samples showed two orders of magnitude lower current density than the reference systems indicating the formation of a barrier layer at the scribe (gap filling of the damage).

The evaluation of healing properties under high potentiostatic polarization is useful mostly when the final application of the coating requires similar conditions as the applied experimental parameters.

9.3.3 Electrochemical Impedance Spectroscopy (EIS)

Electrochemical impedance spectroscopy (EIS) is one of the most used techniques at scientific level in the fields of corrosion and coatings technology and thus its extension and importance in the evaluation of self-healing (anticorrosive) coatings. EIS is a non-destructive test that allows assessment of the degradation (or healing) of the system with time. But more importantly it provides quantitative information of the processes taking place within the system.

Electrochemical impedance spectroscopy is based on electric circuit theory and the description of the different electrochemical processes occurring in the coating-oxide-metal system by a combination of electrical parameters such as resistors and capacitors. The technique uses the description of the behaviour of an electric circuit when an alternating current or voltage is applied as a function of the frequency.

The concept of electrical resistance is well known and is defined by Ohm's law. Resistance is the ability of a circuit to resist the flow of current, mathematically expressed as:

$$R = V/I \tag{9.4}$$

where R is resistance in ohms, V is voltage in volts, and I is current in amperes. However, this simple relationship is limited to one circuit element, the resistor, and it does not represent more complex behaviour that many systems exhibit in the real world. Therefore, the concept of impedance (Z) is introduced. The impedance is a measure of the tendency of a circuit to resist the flow of an alternating electrical current. The equivalent mathematical expression of Eq. (3) for the case of impedance is:

$$Z = V_{ac}/I_{ac} \tag{9.5}$$

This simple and basic equation actually hides some more complicated assumptions and concepts. First, it applies only to the time-varying, alternating, or ac components of the current and voltage. Secondly, it is not sufficient to just

indicate the magnitude of the voltage and the current signals, it must also be expressed how they are related in time, since they are both time-varying ac quantities. Finally, the size and time-relationships nearly always depend on the frequency of the alternating current and voltage.

Figure 9.3 shows a sine wave voltage applied to an electrochemical cell. The response is obtained as a sinusoidal current with certain phase shifting with respect to the perturbation. The response is shifted in time due to the response of this system depending on the combination of resistors and capacitors affecting the kinetics of the process. This time shift is expressed as an angle, the phase angle shift of the current response, or simply the phase angle, φ.

The size of the impedance of this system can be expressed by taking the ratio of the size between the voltage sine wave (in volts) and the current sine wave (in amperes). The signal obtained from the test is the complex impedance ($Z = Z_{re} - j \cdot Z_{im}$). To characterize impedance, Z, both its magnitude or modulus (in ohms), $|Z|$, and phase, φ, as well as the frequency, f (in cycles per second, or Hertz), at which it is measured must be specified together with the amplitude used in the signal input. These three parameters are often plotted on what is known as a Bode plot, shown in Fig. 9.4a, or in the complex impedance form, which is the Nyquist plot (Fig. 9.4b).

The experimental set-up for EIS experiments normally consists of a three-electrode cell: the specimen plate (working electrode), a counter electrode (e.g. Pt wire or mesh, carbon) and a reference electrode (e.g. SCE, Ag/AgCl). The sample is kept under immersion conditions and the impedance test is performed in time. In Fig. 9.5 a scheme of a typical electrochemical cell for EIS measurements is shown.

Commonly the sinusoidal voltage perturbation applied to the electrochemical system is of small amplitude, typically in the range of ±10 mV. The voltage is applied at a given frequency range, usually from 10^5 Hz to 10^{-2} Hz. The instrumentation required to measure the impedance of an electrochemical cell includes a waveform generator to produce the sine wave electrical signal, and a potentiostat to control the potential (Fig. 9.6). These components are controlled by a computer used to run the experiment and to display the results in real time.

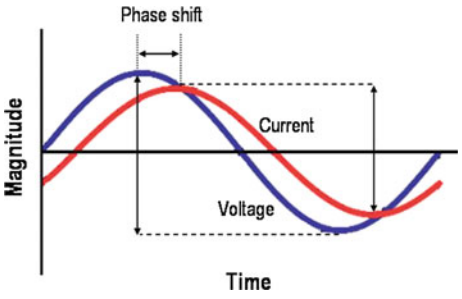

Fig. 9.3 Graphic representation of the current and voltage as a function of time

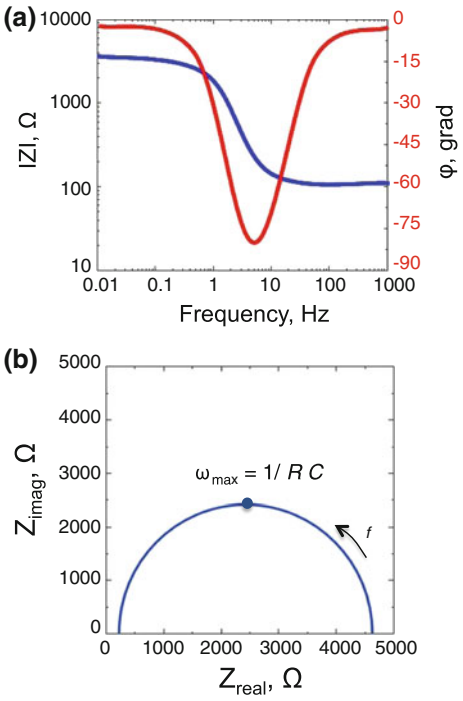

Fig. 9.4 Data representation for impedance data: **a** Bode plot and **b** Nyquist plot

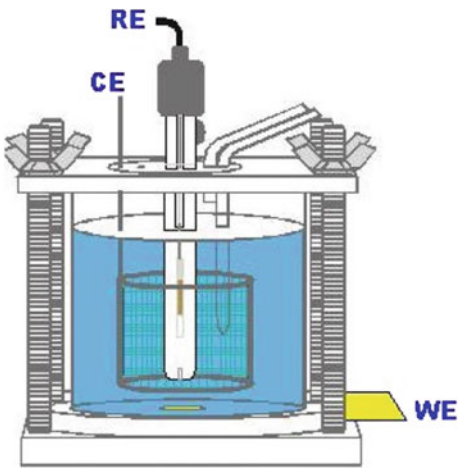

Fig. 9.5 Electrochemical cell used in EIS experiments: *WE*, working electrode; *RE*, reference electrode; and *CE*, auxiliary electrode

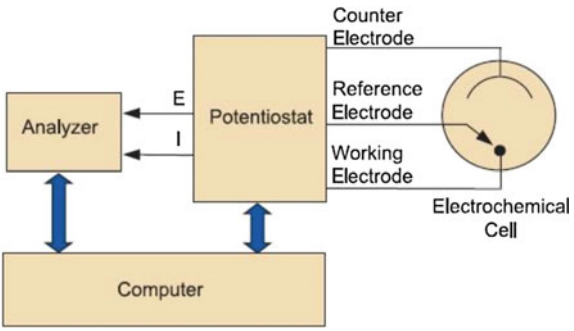

Fig. 9.6 A block diagram of the instrumentation used to conduct EIS measurements

As mentioned at the beginning of this section, EIS is based on electric circuit theory. Therefore the fitting of experimental data with electric equivalent circuits can give extra quantitative information about the system under study. Electrochemical systems such as coated surfaces or corroding metals often behave as simple electronic circuits when an alternating voltage is applied. And, they can be simulated by a set of electric circuit elements such as resistors, capacitors and inductors, which will constitute the *equivalent electric circuit*. This equivalence allows to associate a real chemical-physical process to each of the circuit components.

For example, a simple electrochemical reaction that involves a step of electron transfer such as:

$$O^{n+} + ne- \rightarrow R \tag{9.6}$$

The process can be represented by a simple equivalent circuit which is called Randles' circuit [6]. This circuit is depicted in Fig. 9.7, and consists of a combination of a capacitor and two resistors.

It must be noticed that when an electrochemical reaction occurs at an electrode, at least two associated interfacial processes must be considered, namely:

- the formation of the double layer in the interface, which behaves as a capacitor; and
- the electronic transfer through the interface, which is a faradaic process (resistor).

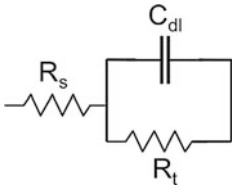

Fig. 9.7 Randles equivalent circuit for a charge transfer-controlled simple electrochemical reaction

This circuit can be used to either represent a simplification of a non-defective coating or a bare corroding metal immersed in an electrolyte solution although such EC simplification rarely describes inhibiting systems [7]. Depending on the electrochemical system the values and meanings of the circuit components are different. Thus, in the case of an intact coating immersed for a short time in an electrolyte, R_S represents the resistance of the electrolyte solution, or uncompensated resistance, between the reference electrode and the surface of the coating. The capacitor, C_{dl}, represents the coating capacitance and is normally represented as C_{coat}, and can be characterized by the thickness and the dielectric constant of the coating material. The resistor, R_t, is associated with the resistance of the coating and generally referenced as R_{pore} (pore resistance). It is also a property of the coating material and varies with its thickness and composition as well as defects.

Corrosion processes are more complex phenomena than just a simple electrochemical reaction. For example in the case of a coating-metal systems immersed for long times, besides the electrochemical reactions (oxidation and reduction), the existence of the coating-metal interface and the simultaneous occurrence of diffusion and adsorption processes should also be taken into consideration. Then a more complex equivalent electric circuit is required to represent the system. For example in the case of corrosion processes occurring underneath the coating, a more specific circuit that can describe this case is shown in Fig. 9.8 [8–12]. The elements of the circuit represent the following characteristics of the system [13]; R_S, the resistance of the electrolyte; R_{pore}, the resistance of the conducting pores in the coating layer; R_t, the charge transfer resistance of the corrosion reaction; C_{coat}, the capacitance of the coating layer; and C_{dl}, the double layer capacitance at the metal/electrolyte interface.

Often better fitting of the equivalent circuit model is obtained by replacing the capacitances in the equivalent circuit presented in Fig. 9.8 with constant phase elements (CPE) [14]. In reality, when studying coated-metal systems, it is difficult to find a pure capacitor behaviour. The deviation from the ideal capacitor can be due to:

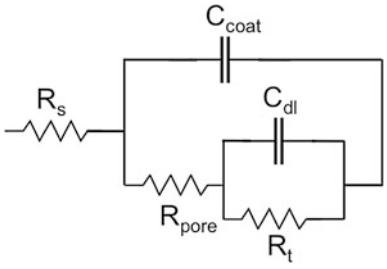

Fig. 9.8 Equivalent circuit of intact coated metal showing corrosion processes underneath the film

- gradients in properties within the coating (laterally and vertically). Such gradients can be caused by resistivity changes [15–17], differences in water takeup [18], porous electrodes [19, 20] to name a few.
- changes in structure such as occurs with layers within a coating or nanoporosity as shown for thin silica layers where the n parameter in the CPE has a linear relation to porosity [21].

However as pointed out by Tribollet and co-workers [15–18] there needs to be a good physical reason for the introduction of CPEs.

Additionally, water uptake, which is calculated through the coating capacitance, is complicated when CPE's are used because of the need to calculate the capacitance from the fitted parameters for the CPE. One equation that has broad acceptance is [22]:

$$C = A\left(\omega_m''\right)^{\alpha-1} \tag{9.7}$$

where A is a constant, ω_m'' is the frequency where the imaginary component of the impedance is a maximum and α is a measure of the capacitive behavior.

One other component worth mentioning is the Warburg impedance which is used to model diffusive behavior at the interface. The use of a Warburg component is generally justified on the basis of the value of the phase angle, where a phase angle of 22.5° or 45° is indicative of a Warburg process [19].

In conclusion, provided a good analysis is performed, information given by EIS can be directly linked to water absorption, kinetics of reaction or absorption, delamination, porosity and adhesion amongst other processes (e.g. diffusion). It is a powerful method for evaluation of (self-healing) anticorrosive coatings since it can provide information about different processes occurring on the system almost simultaneously. For example:

- evolution of the barrier properties of the coatings (water uptake, blistering, delamination)
- corrosion rate at the metal-coating interface
- surface changes due to action of corrosion inhibitors (passivation of the metal surface)

EIS has already been used to assess self-healing anticorrosive (organic) coatings, mainly using total impedance and phase angle as parameter. The main application of this technique has been in extrinsic self-healing coatings using corrosion inhibitors (e.g. loaded nanocontainers with corrosion inhibitors into a sol-gel film [3]). In these tests the normal procedure is the application of an artificial defect reaching the substrate followed by immersion in a corrosive medium (electrolyte). During the experiment it is expected that the corrosion inhibitors will leach out of the coating allowing them to react with the metallic surface at the damage site, decreasing the electrochemical activity, which is observed as a significant increase of the impedance of the system.

EIS has also been successfully employed for liquid encapsulated extrinsic self-healing coatings using two component microencapsulated liquid healing agents [23] or one component microencapsulated healing agent [24] in both cases with excellent results of the use of the technique. In the case of systems using micro-encapsulation, the technique generally shows a more significant increase in impedance than when used for corrosion inhibitor systems due to the restoration of the barrier effect offered by gap filling or full surface coverage [22] in encapsulated concepts and thus major hindering of the electrochemical reactions. EIS has also been recently combined with X-ray microtomography to further understand the mechanisms of protection of single reactive healing agents such as the silyl ester involving delamination and underfilm pitting processes [25].

9.3.4 Odd-Random Phase Multisine Electrochemical Impedance Spectroscopy

As an extension of use of EIS, the odd random phase multisine electrochemical impedance spectroscopy (ORP-EIS) has also been used as a characterization tool for diverse electrochemical processes [26, 27]. ORP-EIS cannot be considered as conventional electrochemical test, but it is included in this section as it provides global (averaged) information of the specimen.

In the previous section the capacity of EIS for the study and evaluation of diverse self-healing systems was presented. A reliable model that describes the system under investigation can only be obtained if the measurement fulfills the conditions of causality, linearity and time-invariance. However, the two last conditions can be difficult to satisfy. EIS measurements are often performed with very small amplitude excitation signals (for reasons of linearity) in the steady state regime of the process (for reasons of time-invariance). As a consequence, the measurements (i) can suffer from poor signal-to-noise ratios and (ii) cannot describe the initial, mostly rapidly evolving, stages of electrochemical phenomena of corrosion processes. Moreover proper fitting of the model to experimental data needs to be achieved, by minimising the residuals between the data and the fit across the whole frequency range [7, 28, 29].

Apart for shorter time measurements ORP-EIS allows measuring the level of disturbing noise, the level of the non-linear distortions and the level of the non-stationary behaviour. The additional information given by this methodology is useful to verify the quality of the measurement. In Fig. 9.9 a typical ORP-EIS spectrum is shown, in which, additional to the conventional impedance data, it is possible to observe the noise level and non-stationary behaviour of the system [30]. As happens with traditional EIS, ORP-EIS becomes a powerful method when combined with the fitting of the data. The additional information helps to reject, accept or improve electrical equivalent circuit models used to fit the conventional impedance spectra. The advantage of the technique has been demonstrated on an electric circuit [27] and the study of corrosion of coated metal [31]. However, it is still scarcely used on the study of self-healing corrosion systems.

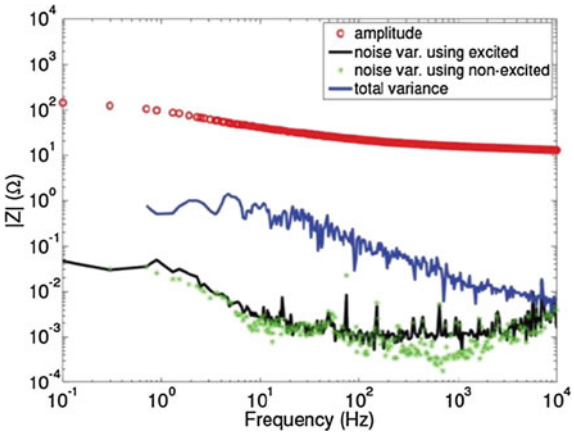

Fig. 9.9 ODR-EIS Impedance spectra plotted on Bode coordinates showing the impedance value (*red*), noise level (*green*), non-stationary behaviour (*black*) and the non-linear behaviour (*blue*) of the corroding metal system

Jorcin et al. [30, 32] applied for the first time this methodology to the study self-healing coatings based on a shape memory polyturethane coating leading to partial physical recovery of the film after macroscale damage. By applying the odd-random phase multisine methodology in contrast to the conventional EIS, it was possible to propose a new equivalent circuit with a more accurate representation of the processes taking place in the coating after damaged. Even though a careful fitting of traditional EIS can also lead to highly accurate equivalent circuits, the ORP-EIS facilitates this task and increases the certainty in the selected EC.

The EC most commonly used circuit to fit damaged coatings (Fig. 9.10) assumes that the impedance data is mainly driven by the defect, representing the coating only as a capacitor C_{coat}. The use of this EC is not based on the overall error

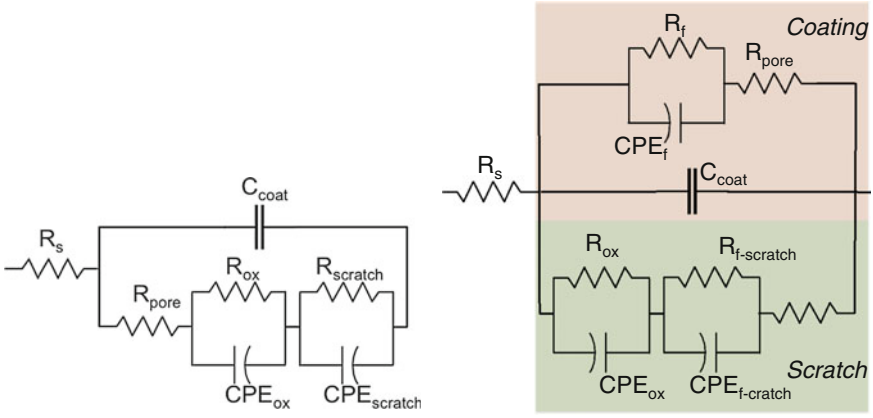

Fig. 9.10 (*left*) Initial equivalent electrical circuit used for the data analysis of the damaged coatings proposed by Bonora et al. [33]. (*right*) New proposition for an equivalent electrical circuit used for the odd-random phase data analysis of the damaged coatings

minimization [7, 24] but on the chi-square, however, it is generally accepted without questioning its validity. When this circuit is applied to fit the odd-random EIS data, a residue (difference between model and experimental data) higher than the stochastic noise of the measurement is observed. This is a clear indication that the equivalent circuit is not well adapted to this electrochemical system probably as a result of a simplification of the physical phenomenon in a damaged coating. Based on this lack of correlation it was possible to propose a new EC consisting in two parts [30]: one related to the organic coating and one related to the phenomena occurring in the artificial defect. The fitting of the data with this new model presented a residue at the level of stochastic noise of the measurement, indicating that all information in the spectrum is taken into account.

The odd-random phase impedance spectroscopy (ORP-EIS) appears as a valuable alternative to conventional impedance methodology for the study of corrosion and self-healing processes. The main advantages are: rapid acquisition of the data and more accurate information to model the system of interest. Nevertheless, analysis of the spectra and the fitting procedure is still tedious and requires a certain level of expertise that makes it not accessible yet for routine research.

9.3.5 AC/DC/AC Accelerated Electrochemical Protocol

Despite the fact that EIS and ORP-EIS can lead to very reliable information about the properties of intact and damaged coatings, they require very long times to assess intact high impedance coatings. In the case of intrinsic self-healing coatings, EIS and ORP-EIS can discern quickly the level of healing when the healed interface is only weakly healed (closed). When the damage interface of the healed coating is of high quality and close to the original network properties non-destructive EIS requires very long times to assess the healing of the scribe. A very recent study with highly efficient intrinsic healing coatings demonstrated that EIS is not capable of detecting any difference between the intact coating and healed coating (macroscale scratches) even after 30 days immersion in corrosive media [34]. In order to detect the healing state (healing degree) the researchers introduced the use of an accelerated destructive electrochemical protocol named AC/DC/AC or ACET. Such technique consists of cycles of EIS measurements/polarization to −2 or −4 V depending on the coating quality/potential relaxation/new EIS to measure the after damage state. [35–38]. When this protocol was applied to self-healing coatings [34] the healed scratches (interfaces) were detected after a number of cycles by a sudden drop of the impedance spectrum. While EIS indicated that the healed coating behaved as a high impedance coating (same behavior as the intact coating) for at least 30 days the AC/DC/AC indicated in three cycles (approximately 12 h) that the damages do act as heterogeneities in the coating even when the healing degree is high (Fig. 9.11). Such a result suggests that healed interfaces can protect damages for long times (at least 1 year as shown in the same article) but that the polymer network at the healed interface remains different from the bulk coating. This first

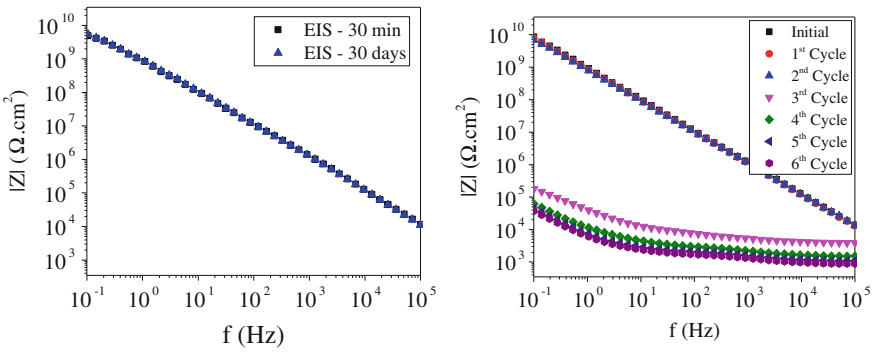

Fig. 9.11 Healed coating after 30 days exposure to electrolyte measured by EIS (*left*) and after 6 cycles of the AC/DC/AC procedure (*right*). (adapted from [34])

time results suggest that the AC/DC/AC technique can be a powerful technique to evaluate healing in intrinsic coatings and potentially even quantify healing degree based on the number of cycles to failure as well as polarization potential applied.

9.4 High-Throughput Screening Techniques

In the previous section the most common electrochemical methods to evaluate the efficiency of self-healing systems were introduced. In general, these techniques require testing times ranging from hours (in the case of electrochemical studies) to weeks (for accelerated laboratory testing, mass loss testing) or even years (in the case of outdoor exposure testing) and produce data on only one system of interest at a time. Hence, if a broad range of systems is to be investigated, more rapid means of evaluating their performance need to be found. This is typically an issue for the research focused on development of new corrosion inhibitive coatings. Restrictions on using Cr(VI) compounds for corrosion protection has forced an increase in the effort to search for equally efficient substitute inhibitors. Up to now the research of alternative corrosion inhibitors for all sorts of metals is still an ongoing topic. Within the development of new protective coatings we can identify five stages or milestones (Fig. 9.12):

- selection of alternative inhibitor candidates
- evaluation of their intrinsic efficiency
- incorporation into the coating
- total performance evaluation
- final optimization of delivery kinetics

In all these steps the main problem, apart from finding the perfect inhibitor, is that it is a very time consuming process, especially when thousands of inhibitor candidates have to be tested. For this reason the introduction of high throughput

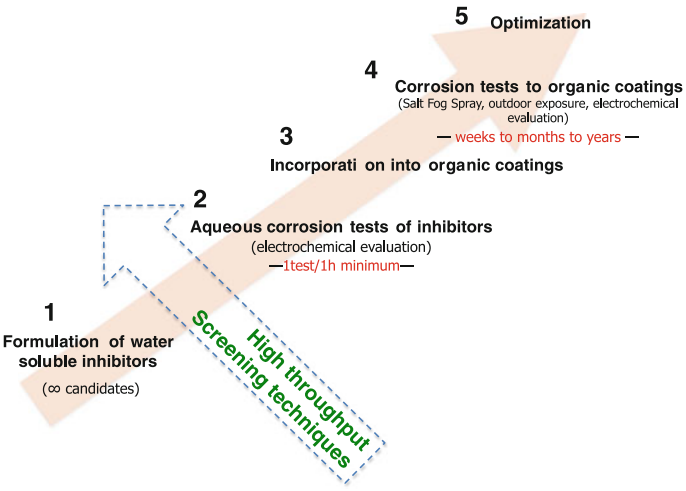

Fig. 9.12 Scheme presenting the milestones to develop corrosion inhibitive coatings [41]

techniques for inhibitor selection is a very necessary step previous to traditional aqueous corrosion tests. It is needed to test the efficiency of a large number of chromate-free alternative inhibitors and to be able to provide a shortlist of candidates in a reasonable time. Furthermore, due to the reliable and efficient performance of chromate-based inhibiting technologies, attempts to find a 'direct replacement' have largely failed, and therefore, present day approaches aim to develop 'multifunctional' corrosion inhibitors, which have the ability to passivate both anodic and cathodic reaction sites at the metal surface. Inhibitor development and evaluation approaches therefore require a large number of experiments if a systematic survey of potential cathodic, anodic and combined (multifunctional) inhibitors is to be performed [39, 40]. Then, high-throughput or rapid screening methods need to be used for assessing inhibiting efficiency of a broad range of potential inhibitors.

In this section the development of rapid screening techniques for high-throughput testing of inhibitors is described

Multi-electrode arrays have been introduced in recent times as valuable methods to carry out corrosion measurements [42–44] and high-throughput testing of corrosion inhibitors [45–49].

In the approach proposed by Taylor et al. [46], identical pairs of metal wires were placed into a large number of separate reaction wells. The experiment consisted of polarizing one of the electrodes with respect to the second pair which is held at a potential corresponding to the open-circuit potential of the metal. The current between each pair was monitored and used to measure the linear polarisation resistance (LPR) from which the corrosion rates can be calculated.

Muster et al. [41, 50] presented an adaptation of the multiple-electrode method that allowed the simultaneous investigation of several metals in one solution. Pairs

of metals were immersed into various inhibitor solutions at relatively low polarization. The current flowing between the individual electrodes of each metal pair was measured. The current exchange between the individual electrodes of the same metal then was expressed in inhibitor efficiency with respect to that in uninhibited solutions.

Other main differences with respect to Taylor and Chambers approach are:

- no reference electrode is used to fix electrode potentials of the metals
- a blank sample is used as a control for each inhibitor evaluation

Electrochemical methods are usually not carried out in the absence of a reference electrode. However, for the rapid screening of multifunctional corrosion inhibitors, the omission of the reference electrode offers the benefit of simplicity whilst retaining the key information regarding inhibition.

High-throughput screening methods reduce the experimental time significantly. For example, in the work of Taylor and Chambers [45, 46] potential corrosion inhibitors and their synergistic combinations for aluminium alloy AA2024 were studied. The inhibition characteristics of 50 separate chemistries were assessed simultaneously. The test using direct current (DC) polarization in the multiple-electrode system was performed within 9 h while for electrochemical impedance experiments for the same number of inhibitors at least 10 days of measurements was needed.

In addition to electrochemical techniques that aim to determine the corrosion current, or potentiostatic current as above, high throughput studies of corrosion inhibition have also been applied to the detection of chemical changes. These techniques are non-electrochemical, high-throughput screening methods. These methods are based on fluorimetric [45, 51] and spectroscopic measurements [52]. They are used to determine the concentration of chemical species in solution.

A different type of method for high-throughput screening is based on micro-fluidic approaches [53]. These differ from the multielectrode in that only one metal can be studied in the one test. The metal is exposed to a range of aqueous corrosion inhibitors and concentrations via micro-fluidic channels. The sample is visually inspected and solutions are chemically analyzed. Another non-electrochemical high-throughput test employs arrays of wells which are filled with inhibitor-doped solutions and after exposure the bottom wells are then examined by digital micrograph analysis [54].

9.5 Local Electrochemical Techniques

In Sect. 9.3, general electrochemical methods were presented. These methods are characterized by having the sample of interest as working electrode. The obtained results provide averaged information of the electrochemical processes taking place on the entire surface of the working electrode. In this section we examine localised electrochemical techniques.

9.5.1 Electrochemical Microcapillary Cell

The electrochemical microcapillary cell is a technique used to perform conventional electrochemical measurements (open circuit potential measurements, potentiodynamic polarization and EIS) on areas with dimensions in the micrometer range [55, 56]. In general the microcapillary cell is a powerful technique since it allows performing electrochemical measurements on very small surface areas, in the micrometer range.

The microcapillary cell is based on the miniaturization of the standard three-electrode cell setup. For this, the area of the working electrode is reduced by using a glass microcapillary which holds a droplet of the electrolyte on the sample surface. The most common sizes of the tip of the capillary are found between 10–100 μm for corrosion research, but can be even less. The droplet of electrolyte can be held in position in two different ways: free droplet and silicone rubber gasket [57]. The silicon gasket provides a cushion while approaching and reaching the sample and it avoids leakage of electrolyte. The silicone with its high deformability shapes to the roughness of the surface. In any case, the wetted area on the sample surface defines the working electrode.

In Fig. 9.13 a scheme of the components of the microcapillary cell technique is shown. The setup consists of micro-electrochemical cell (3-electrode cell), microscope, camera, potentiostat and computerized controller. The microscope and camera enable a fast and precise positioning of the microcapillary on the desired spot of the sample surface. The components that will determine the resolution and quality of the electrochemical measurements are mainly:

- The potentiostat. A high resolution potentiostat is required. The current detection limit of the potentiostat will determine the resolution of the measurements. Currently modern instruments have a lower detection limit for the current down

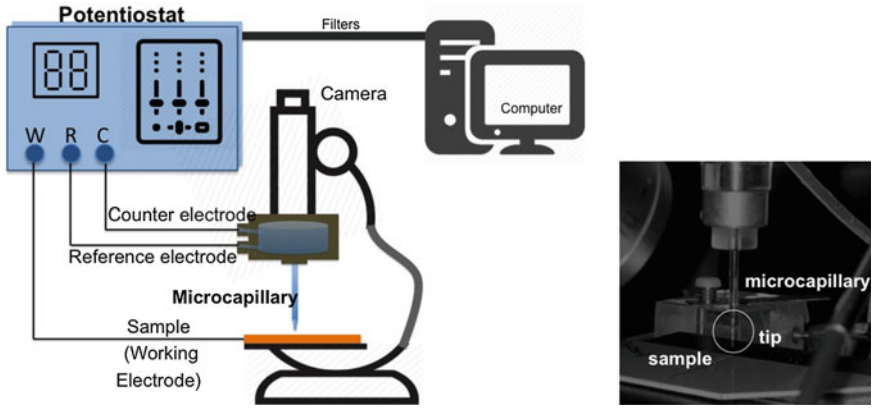

Fig. 9.13 (*left*) Schematic of the electrochemical microcapillary cell setup. (*right*) Detail of the microcapillary approaching the sample surface

to pA and fA levels. Furthermore, adequate isolation and filters to reduce noise influencing the measurements is required.

- Microcapillary. Preparation of the microcapillary consists of "pulling" a glass capillary until the desired shape and diameter is obtained. The final size of the capillary is achieved by careful grounding and polishing of the capillary tip. Afterwards, the silicone gasket is applied. The final inner diameter of the capillary will influence the limiting current density during the measurements. It is important to take into account this factor when planning a experiment. For example, a current density of 10 $\mu A/cm^2$ corresponds to a capillary of 1 μm diameter (exposed area). This is equivalent to corrosion currents in the order of 10 fA [57].

The electrochemical microcapillary cell is a very attractive technique to study the effect of microstructural features on the corrosion mechanisms of metal alloys. The microcapillary cells have been successfully used to the study of the local behaviour of intermetallics in aluminium alloys [58–60] and pit initiation of steels [61–63].

In this sense, the microcapillary cell can be used to study the protection mechanism of corrosion inhibitors for individual phases or intermetallics from the metal alloy. Some works have been done focusing on rare-earth corrosion inhibitors and their cathodic-type behaviour for AA2024 alloy.

Birbilis et al. [64] studied the protection mechanism of AA2024 alloy offered by cerium dibutyl phosphate ($Ce(dbp)_3$). Taking advantage of the capabilities of the microcapillary cell, it was possible to perform potentiodynamic measurements on individual intermetallics and to study their behaviour in presence and absence of the inhibitor. Cathodic polarization curves on the main cathodic phases (Al_2Cu, Al_7Cu_2Fe, $Al_{20}Cu_2Mn_3$, and Al_3Fe) showed that the $Ce(dbp)_3$ effectively inhibits oxygen reduction on each of them. Interestingly, anodic polarization curves measured for anodic phases (Al_7Cu_2Fe and Al_2CuMg) demonstrated that the inhibitor is able to stabilize the passivity of these phases. This work suggested that $Ce(dbp)_3$ acts as a mixed inhibitor offering cathodic and anodic inhibition for the AA2024 alloy. It may effectively inhibit localized corrosion owing to its mixed nature, providing retardation of the oxygen reduction reaction upon noble intermetallics and concomitant retardation of dissolution of phases that may be prone to attack.

In the work of Andreatta et al. [65] the localized corrosion inhibition of $CeCl_3$ was investigated for clad AA2024. In this case the research focused on the behaviour of areas containing Fe-rich intermetallic compounds and areas without inclusions (matrix). Microcapillary based potentiodynamic polarization evidenced that the deposition of Ce-species occurs on the entire sample surface being affected by the alloy microstructure. Moreover, it is activated by alkaline etching of the substrate. The deposition takes place preferentially at the sites of intermetallics due to their cathodic behaviour and to local alkalinization associated with cathodic reactions. It was possible to demonstrate that the amount of Ce detected at the sites of intermetallics is larger than on the matrix.

More recently, the microcapillary cell has been used to characterize the protective layer formed in a scratch by inhibitor released from the coating after it is

damaged. In this work by Recloux et al. [66], benzotriazole (BTA) inhibitor was incorporated into a silica mesoporous thin film as pretreatment applied on an AA2024 alloy sample. The acquisition of local anodic polarization curves with the microcapillary cell on the bare metal exposed in the scribed coating was used to monitor the formation of a passive film by the BTA within the defect. The results demonstrated that the inhibitor was directly released from the mesoporous pretreatment once the top coat was damaged and acted rapidly to protect the bare metal and to delay the initial stage of corrosion phenomena.

It is clear that this type of information and conclusions are not accessible from conventional (macroscopic) potentiodynamic experiments. The microcapillary cell is a powerful method for localised electrochemical measurements and to establish correlation between corrosion/inhibition mechanisms and microstructural features at metal surfaces.

Nevertheless, the electrochemical microcapillary cell technique also presents several drawbacks or precautions:

- risk of crevice corrosion at the silicon periphery of the capillary
- requires a large number of measurements to assure the reproducibility of the results
- possibility of contamination of the solution during the measurement
- small size of the microcapillary can affect the transport of species to the substrate, such as oxygen and protons resulting in diffusion limited corrosion behaviour
- problems with high ohmic resistance between working and counter electrode can occur. The choice of an appropriate geometry of the cell will minimize this issue.

9.5.2 Scanning Vibrating Electrode Technique (SVET)

The SVET technique produces in situ measurements with high spatial resolution and provides valuable information on the behaviour of the corroding system at a microscopic level [67, 68]. The SVET offers the possibility of mapping variations in the ionic current densities in the micrometric range facilitating the location of anodic and cathodic zones (related to corrosion processes). This technique is based on the detection of electric fields generated in a solution due to ionic concentration gradients. The electric field is zero when the solution is at rest, but if there is a gradient of concentration caused by a source of ions, a variation of potential in the solution occurs. Ionic flows can arise from corrosion processes on a metal. The oxidation reactions occurring at anodic sites on a metal surface in contact with an electrolyte cause electrons to flow through the metal substrate to adjacent cathodic areas. This flow of electrons through the metal is supported by a flow of ionic current in the electrolyte, which in turn causes potential gradients to exist in the solution close to sites of localized corrosion. Figure 9.14 depicts a scheme of the

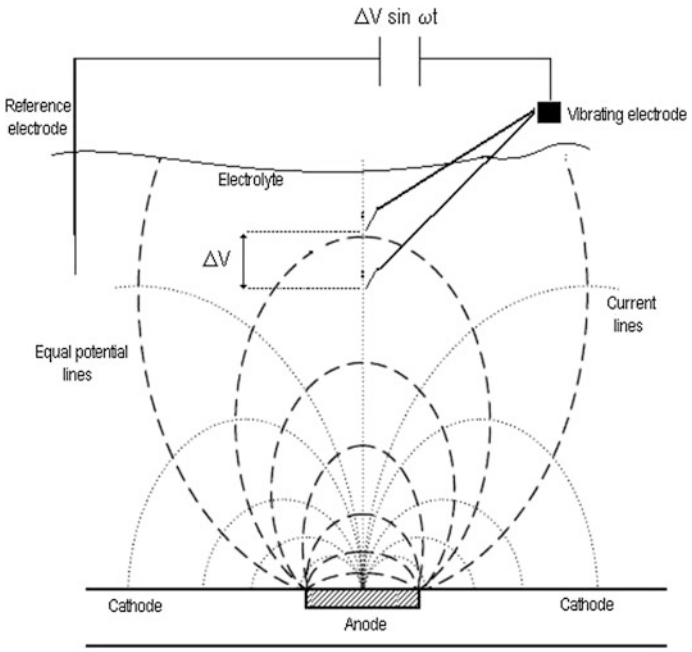

Fig. 9.14 Schematic representation of the operation principle of the SVET technique

distribution of equal-potential and current lines during a corrosion process and the operation principle of the SVET.

The SVET uses a vibrating microelectrode that scans the surface to measure these gradients in situ. Measurement is made by vibrating a fine tip microelectrode a few hundred microns above the sample, usually in a plane perpendicular to the surface. The electrochemical potential of the microelectrode is recorded at the extremes of the vibration amplitude, resulting in the generation of a sinusoidal AC signal (cf. Fig. 9.14). Then this signal is measured using a lock-in amplifier, which is tuned to the frequency of probe vibration. The measured potential variation, ΔV, can be related with the ionic currents (I) by use of the equation [7, 69]:

$$I = \frac{E}{\rho} = \frac{1}{\rho}\frac{\Delta V}{\Delta r}. \tag{9.8}$$

where E is the electric field measured between two points of the solution, ρ is the resistivity of the solution, and Δr the distance between the two extremes or vibration amplitude of the microelectrode.

The resulting signal, which is a measure of the DC potential gradients in solution, can be converted to current density by a calibration procedure. This consists of placing the vibrating microelectrode at a known distance from another electrode that acts as source of a given constant current. Then the potential measured by the

SVET probe at determined distance from the source corresponds to a known current. The potential (V) measured in each point can be related to the current intensities (I) of the processes occurring at the metal surface by Ohm's Law, using the following equation:

$$V = \frac{I\rho}{2\pi d} \tag{9.9}$$

where ρ is the resistivity of the solution, and d the distance between the point of measurement and the source of the current. The calibration is valid for the solution used and while the amplitude and the frequency of the vibration remain unaltered [70].

The scanning vibrating electrode instrument is basically constituted by:

- The electrochemical cell (detail in Fig. 9.15)
- The piezo-oscillator system which produces the vibration of the microelectrode
- Two lock-in amplifiers that measure and filter the signal produced in the probe.
- Tri-axial piezoelectric motors to control with precision the movement and the position of the vibrating probe
- Computer, interface and display system

The SVET microelectrode consists of a platinum/iridium (Pt/Ir: 80 %/20 %) wire insulated with paralene C® and arced at the tip to face the metal. The tip is platinized to form a small spherical platinum black deposit of 10–20 μm diameter. An image of the tip after platinization is shown in Fig. 9.15.

A map of current distribution can be obtained by making a grid of points and measuring at each point the potential difference while scanning in a plane parallel to the surface of the sample. The SVET is therefore a technique able to make in situ measurements of the localised corrosion activity occurring at the surface of the sample. Figure 9.16 shows an example of the application of the SVET for measuring the distribution of anodic and cathodic activities on AA2024 alloy sample during immersion in chloride solution.

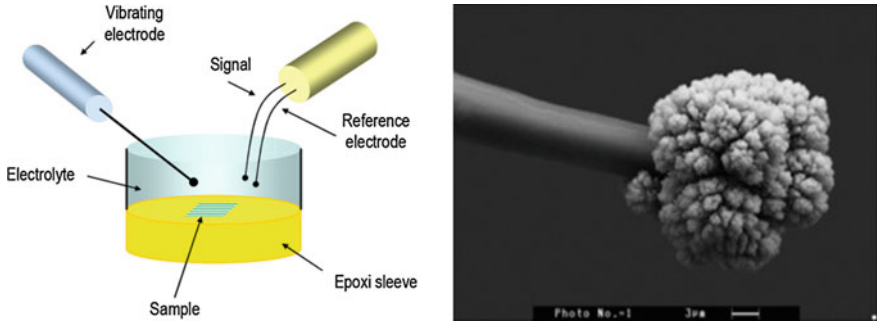

Fig. 9.15 (*left*) Configuration of the electrochemical cell employed in the SVET experiments (*right*) Image of the SVET microelectrode tip after platinization

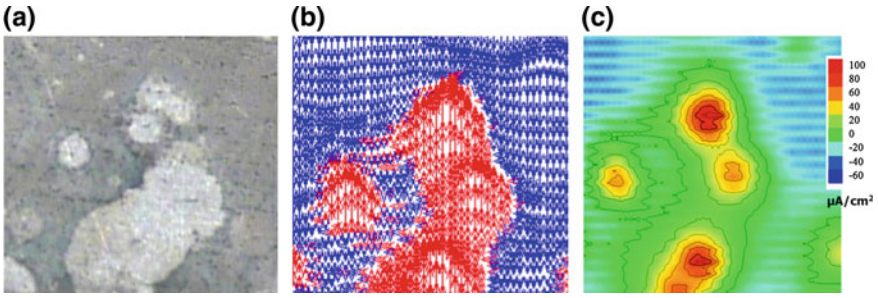

Fig. 9.16 **a** Image of AA2024-T3 sample after 2 days immersed in 0.05 M NaCl solution (image obtained while in solution). Scale 1 mm × 1 mm. **b** Vector map of the SVET data representing the direction of ionic currents. **c** Current density map of the surface. Anodic and cathodic currents can be correlated with the aspect of the sample in (**a**)

One of the important advantages of the SVET is that it is not a destructive method, in the sense that it allows to visualize corrosion activity occurring on the same sample surface during immersion [71]. The SVET is currently one of the most extended scanning micro-electrochemical techniques applied for corrosion research.

SVET measurement is widely used for analysis of corrosion inhibitor performance [72, 73]. In this case the bare metal substrate is immersed in the solution containing the inhibitor under study. Sequential SVET maps are obtained with immersion time to monitor the corrosion activity on the surface in situ.

Inspired by the high-throughput concept, a fast screening of the corrosion inhibitors by SVET measurements has also been proposed [74, 75]. It consists of a multi-electrode cell with a range of metal wires embedded in insulating material. Then the inhibition performance of the inhibitor for each metal wire is monitored all at the same time by using SVET. It can be used as preliminary testing when a large number of metals and corrosion inhibitors have to be tested.

With the emerging interest on finding new, environmentally friendly inhibitors and novel inhibitor controlled release concepts, the number of publications using the SVET has increased significantly in the last years [76–78]. With this technique it is possible to monitor the corrosion or inhibition activity in a coating defect. Therefore it is a useful and straightforward method to evaluate the performance of self-healing polymeric coatings [24, 79].

9.5.3 Selective-Ion Electrode Technique (SIET)

The SIET consists of a potentiometric micro-probe that measures the concentration of specific ions at a quasi-constant distance (at micrometer range) over the surface of interest. Potentiometric micro-probes have been used for biological applications for a long time now. Profiles and gradients of concentrations of Ca^{2+}, Mg^{2+}, K^{+}, Na^{+}, NH_4^{+}, Cl^{-} determined by potentiometric micro-sensors above biological

specimens have been reported in numerous publications [80–83]. It is not until recent years that the SIET technique has been used to monitor specific ions in real corroding systems. The first time, it was applied for mapping local activity of Mg^{2+} and H^{+} over the surface of a Mg-based alloy in chloride-containing solution [84].

The main components of a SIET device are: an ion-selective microelectrode, a reference electrode (e.g. Ag/AgCl mini-electrode), 3D computerized stepper-motors systems, a camera to control the location of the microelectrode over the sample.

The microelectrode consists of a glass-capillary filled with a selective ionophore-based oil-like membrane. The microelectrode also includes an inner reference electrolyte and the reference electrode Ag/AgCl wire. The diameter of the glass-capillary microelectrode varies from 0.1 to 5 μm. This type of electrode is highly fragile and have limited life time (<1 day). Furthermore, the detection limit is biased by the flux of primary ions from the ion-selective membrane and inner reference electrolyte. Recently, more robust designs have been introduced. They are based on solid-contact ion-selective microelectrodes which do not require an inner reference solution [85–89].

The potential measurements are correlated to the ion concentration (activity) by the Nernst equation:

$$E_i = E_i^0 + \frac{RT}{Fz_i} ln a_i \tag{9.10}$$

where F is the Faraday constant, R is the universal gas constant, and T is the absolute temperature.

Before and after measuring a sample the ion-selective microelectrode has to be calibrated. The calibration consists of recording the potential E_i versus time dependence with sequential increase of ion activity, a_i. This also allows to check the stability of the potential measurements, the drift and the time response. More details about potentiometric measurements can be found in several reviews [90, 91].

SIET mapping has been used in several studies to evaluate corrosion inhibitor efficiency and mechanism [92, 93]. For example, the corrosion processes on AZ31 alloy coated with hybrid sol-gel was studied in NaCl solution containing three different potential inhibitors by Karavai et al. [94]. Localized measurements of pH and Mg^{2+} concentration at microdefects of the sample showed that it was possible to obtain complementary information of electrochemical reactions inside the defect.

9.5.4 Scanning Electrochemical Microscope (SECM)

The SECM is a non-optical scanning microscopic instrument which is included in the group of scanning probe microscopies (SPMs) [95]. The SECM is based on the reaction that occurs on the surface of a microelectrode immersed in the electrolyte solution. The microelectrode is scanned in close proximity to the sample surface to

characterize the topography and/or redox activity of the microelectrode/sample interface [96]. This latter feature is very important, because it allows SECM to gain information about reactions that take place in the solution space between the tip and the sample, as well as on those occurring on the surface of the scanned sample. The SECM has become a very powerful technique for probing a great variety of electrochemical reactions, due to the combination of its high spatial resolution and its electrochemical sensitivity. Its capability for the direct identification of chemical species with high lateral resolution is of great interest in the study of corrosion processes [97].

Prior to explaining the operation and the response of the SECM, it is necessary to understand the behaviour of the microelectrode inside the electrochemical cell. Let's consider the case where the microelectrode is immersed in a solution containing an electrolyte and a reducible species, R. When a potential sufficiently negative is applied to the microelectrode, the reduction of the specie occurs at the surface of the microelectrode:

$$R^{n+} + ne- \rightarrow O \tag{9.11}$$

If this reaction is kinetically controlled by the diffusion of R from the bulk of the solution to the electrode surface, the current decays due to the formation of a diffusion layer of R around the electrode, and attains a steady-state value rapidly given by:

$$\boldsymbol{i_{lim}} = 4nFDca \tag{9.12}$$

where F, is the Faraday constant; a, the microelectrode radius; D, the diffusion coefficient of the reducible species; and, c, its concentration.

A steady-state current results from the constant flux of R to the electrode surface due to an expanding hemispherical diffusion layer around the microelectrode (Fig. 9.17).

The measurements at a SECM microelectrode are not affected by stirring or other convective effects. In SECM measurements, the proximity of the tip to the substrate is the perturbation that constitutes the microelectrode response [96]. If the microelectrode is brought to the vicinity of an insulating substrate, the steady-state current that flows through the tip, tends to be smaller than i_{lim} (Fig. 9.18). This is a result of the insulating substrate partially blocking the diffusion of A^{n+} towards the tip. The current at the tip becomes smaller when the tip is closer to the substrate, and tends to zero when the distance between tip and substrate, d, approaches zero. This effect is known as *negative feedback*. In contrast, if the tip is close to a conductive substrate at which the oxidation reaction of A can occur (Fig. 9.18). Then a flux of A^{n+} from the substrate to the tip occurs, in addition to some flux from the bulk solution towards the tip. This effect leads to an enhancement of the current at the tip, i_{tip}, which is higher than i_{lim}. This effect is known as *positive feedback*.

Then by using A^{n+} as electrochemical mediator, the nature of the substrate (conductive or insulating) can be established. The SECM technique operating in

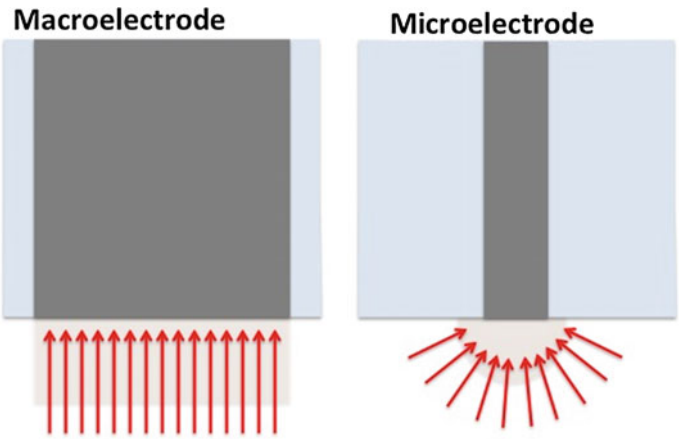

Fig. 9.17 Scheme of the geometry and diffusion field for (*left*) conventional macro-electrode, and (*right*) microelectrode. They present linear and hemispherical diffusion layer respectively

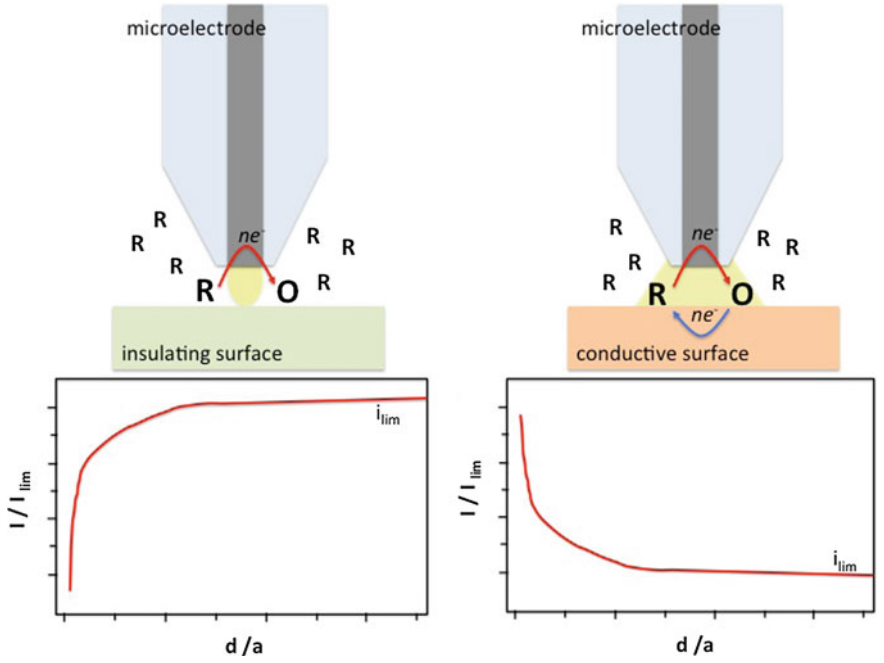

Fig. 9.18 Basic principle of SECM: (*left*) Negative feedback: The tip is placed near an insulating substrate which hinders the diffusion of species A^{n+}. (*right*) Positive feedback: The tip is located near a conductive substrate where the oxidation of species A occurs

this mode provides an excellent tool for the in situ study of film growth on various materials. Such is the case for the formation of a passive layer by corrosion inhibitors. Several works have been published in the study of organic inhibitors for the protection of copper [98, 99]. SECM was used to follow the transition of the copper surface from conducting to insulating as film growth proceeds. A scheme showing this effect is presented in Fig. 9.19. A sequence of approaching curves of the SECM microelectrode towards the metal (copper) is recorded. It represents the transition of the metal from active to passive with the time of immersion in the solution containing the inhibitor.

When studying with the SECM, organic corrosion inhibitors such as mercatobenzimidazole, benzotriazole or similar, it should be noted that often contamination of the microelectrode by the deposition of the inhibitor on it, may occur. Measurements should be performed with caution and regular checking of the state of the electrode is needed. There is no report so far of using the SECM for the evaluation of inorganic chromate-free inhibitors for the protection of aluminium and steel alloys.

Another way of operating the SECM is the generator-collector mode. In this case the tip current is used to monitor the flux of electroactive species generated or consumed by the metal substrate. The microelectrode is polarized at certain potentials where a redox reaction of one of the species takes places. This configuration has been applied to determine concentration profiles of species involved in the corrosion processes [100]. Iron, zinc and oxygen profiles have been monitored when corrosion is taking place on bare metals and defective coatings [101–103].

Recently this SECM operating mode has been applied for the evaluation of self-healing processes. In this case measurements are based on monitoring changes of dissolved oxygen concentration in the solution at the proximity of the substrate. The reduction of oxygen is commonly the cathodic reaction of corrosion processes in neutral/alkaline solutions. A consequence of this is the local depletion of

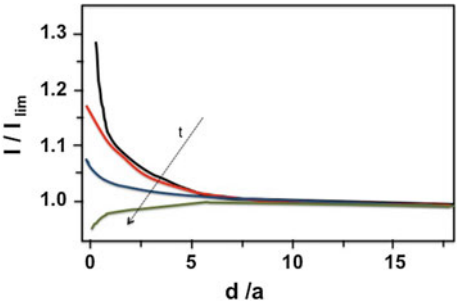

Fig. 9.19 Plot representing approaching curves of the microelectrode toward the metal surface at different immersion times. By the formation of a passive layer by the inhibitor action, a change of the response of the metal from conductive to insulating is detected. X axis: normalized distance (d/a = distance/electrode radius). Y axis: normalized current (I/I_{lim} = measured current/limiting current)

dissolved oxygen concentration in the solution near the cathode area (Fig. 9.20). This is an indirect way to follow the spontaneous corrosion processes occurring on a metal system and their depletion by the action of the healing process. This mode was used to evaluate the healing efficiency of polymer healing in a shape-memory type of coating for protection of an aluminium substrate [104]. Also this operation mode was used to study an autonomous healing system consisting of encapsulated healing-agent incorporated into organic coating for protection of the underlying metal substrate [105, 106].

The SECM oxygen sensing measurements are very interesting for corrosion research, however the results (profile concentration of oxygen) should be carefully discussed. While reducing oxygen at the SECM tip, two undesired processes will take place at the proximities of the microelectrode: consumption of dissolved oxygen and increase of pH by the generation of OH^- ions. These processes can have an impact on the corrosion processes taking place on the metal substrate, affecting the kinetics and the formation of corrosion products. The SECM measurement by itself can influence the natural corrosion mechanism under study. This undesired effect has been pinpointed by electrochemical simulation [107] and the analysis of the corrosion products [108]. The magnitude and impact of the undesired effect depends on: the proximity of the tip to the substrate and the duration of the experiments. When performing the experiments, short-time measurements and a

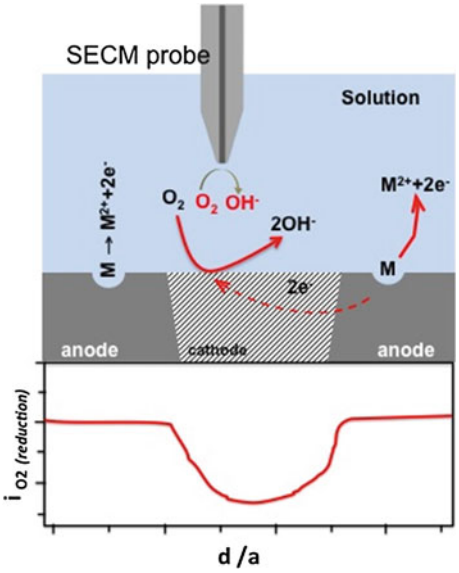

Fig. 9.20 (*top*) Diagram showing the anodic and cathodic reactions (oxygen reduction) on a corroding metal. The SECM microelectrode is polarized at a potential corresponding to the reduction potential of oxygen. (*bottom*) SECM line scan of the microelectrode across the metal surface. It shows the depletion of current when scanning over the cathodic region where less oxygen is available for the reduction reaction at the microelectrode

large tip-substrate distance is desired. The SECM oxygen sensing mode is a valuable method for *qualitative* indication of corrosion activity on the metal surface, but quantitative data should be carefully interpreted.

In general the main components of the scanning electrochemical microscope are:

- The tip movement and position controller, which is the SPM component.
- The electrochemical cell, which is formed by the tip, the counter electrode, the reference electrode and the substrate that, occasionally, can act as second working electrode.
- The bipotentiostat, which constitutes the SECM electrochemical setup together with the electrochemical cell. The bipotentiostat allows to polarize microelectrode and sample.
- Computer, interface and display system.

The most common microelectrode used for corrosion research is a platinum wire embedded in a glass capillary, resulting in a microdisc electrode. The diameter size of the electrode can vary from 1 to 25 μm.

SECM is a more versatile technique when compared to SVET or the microcapillary cell since it provides higher resolution (wide range of microelectrode sizes) and chemical selectivity at the same time to monitor electrochemical processes occurring on the surface. When performing SECM measurements several facts needs to be considered:

- resolution of the measurement depends on the microelectrode dimensions and tip-sample distance,
- possible contamination or poisoning of the microelectrode. It is important to check the state of the tip after experiments,
- undesired influence of the SECM measurement on the system to be studied, The redox processes occurring on the microelectrode can affect the electrochemical processes taking place on the sample.
- select the adequate scan rate to assure limiting steady-state during measurement

9.5.5 Local Electrochemical Impedance Spectroscopy (LEIS)

SVET and SECM are based on the measurements of events or processes taking place between the probe and the specimen. A disadvantage of both these techniques is that this information may be disturbed by noise or limited response from the substrate, and the impossibility to obtain information of the processes underneath a coating. Local Electrochemical Impedance Spectroscopy (LEIS) appears an alternative where it is important to have direct information of the response of the substrate under different conditions such as during a healing event.

The LEIS technique is based on the hypothesis that the local impedance can be generated by measuring the AC-local current density in the vicinity of the working electrode in a three-electrode cell configuration. This was introduced by the Isaacs group in the 1990s [109]. Quantitative information was achieved by using a dual microelectrode for sensing the local AC-potential gradient, and therefore the local current by direct application of Ohm's law. The use of a multichannel frequency response analyzer also allows for the simultaneous measurement of global and local response of the specimens. The resolution of the technique depends on the size of the electrodes used in the bi-electrode probe to sense the local potential and the spacing between the electrodes. More detailed information about the fundaments of LEIS can be found in the recent review by Huang et al. [110].

The first applications of LEIS method were in the study of corrosion processes and focused on the investigation of localized delamination of coatings. As an example, Jorcin et al. in 2006 [32] mapped local electrochemical impedance which allowed them to observe and quantify the delamination process beneath the steel/epoxy-vinyl primer interface. An interesting observation was that the delaminated surface area measured by LEIS was significantly higher than that observed by visual examination of the systems. These results pointed out that LEIS is a powerful technique for visualizing, with high accuracy, the zones of coatings where adherence to the metal substrate has been lost.

The use of LEIS to evaluate the local efficiency of a healing mechanism against corrosion is becoming more common in recent years. Several works have demonstrated the capabilities of LEIS method for evaluation of corrosion inhibitor performance [111, 112]. Snihirova et al. [113] presented a new smart anticorrosion system for AA2024, based on the incorporation of encapsulated inhibitor into a coating. Controlled delivery was triggered by local changes of pH induced by the corrosion processes. Conventional EIS and local impedance spectroscopy were used to evaluate the efficiency of the systems as function of the active inhibitor employed and their incorporation into the coating.

The resolution of the LEIS technique depends on the size of the electrode/sensor and the distance between the electrode and the sample. The ultimate resolution achievable is constrained by the sensitivity of the potential measuring circuitry. Measurement sensitivity in the order of 1 nV limits the resolution to the micrometer range [110].

9.6 Conclusions

This chapter describes several global and local electrochemical techniques used for the evaluation and characterization of novel protection approaches based on extrinsic and intrinsic self-healing concepts.

Potential measurements, potentiodynamic experiments and electrochemical impedance spectroscopy (EIS) are the most commonly used methods used for corrosion and self-healing research. These global methods provide kinetic and

mechanistic information of the self-healing processes. Apart from these traditional techniques some newer methods based on EIS have been proposed to obtain faster and more accurate information about the healing degrees and process such as the odd-random EIS and the AC/DC/AC protocol.

High-throughput techniques have also attracted considerable interest due to their powerful use for fast screening of a large number of samples. This is tremendously useful for evaluation of potential corrosion inhibitors of potential use in self-healing concepts.

In order to obtain local information about the evolution of damage and protected or healed damage local electrochemical techniques with spatial resolution have been proposed. Within this group micro-capillary cell, scanning vibrating electrode technique (SVET), selective ion-electrode technique (SIET), scanning electrochemical microscope (SECM), and local electrochemical impedance spectroscopy (LEIS) are the most common. Even though these techniques have so far only been used to obtain pseudo-quantitative information about the healing degree they have the potential to be used for more quantitative studies of the healing processes themselves.

There is no doubt that electrochemical evaluation of self-healing processes is considered a key requirement to understand the healing mechanisms and to evaluate the corrosion performance of new developments. Nevertheless, these studies should always be supported by dedicated complementary surface, optical and/or physical chemical analysis.

References

1. V. Sauvant-Moynot, S. Gonzalez, J. Kittel, Self-healing coatings: an alternative route for anticorrosion protection. Prog. Org. Coat. **63**(3), 307–315 (2008)
2. S.R. White et al., Autonomic healing of polymer composites. Nature **409**(6822), 794–797 (2001)
3. D.G. Shchukin et al., Layer-by-layer assembled nanocontainers for self-healing corrosion protection. Adv. Mater. **18**(13), 1672–1678 (2006)
4. K. Aramaki, The inhibition effects of cation inhibitors on corrosion of zinc in aerated 0.5 M NaCl. Corros. Sci. **43**(8), 1573–1588 (2001)
5. S.H. Cho, S.R. White, P.V. Braun, Self-healing polymer coatings. Adv. Mater. **21**(6), 645–649 (2009)
6. J.E.B. Randles, K.W. Somerton, Kinetics of rapid electrode reactions. Part 3. - Electron exchange reactions. Trans. Faraday Soc. **48**, 937–950 (1952)
7. S.J. Garcia et al., Unravelling the corrosion inhibition mechanisms of bi-functional inhibitors by EIS and SEM-EDS. Corros. Sci. **69**, 346–358 (2013)
8. J.M. Hu, J.Q. Zhang, C.N. Cao, Determination of water uptake and diffusion of Cl- ion in epoxy primer on aluminum alloys in NaCl solution by electrochemical impedance spectroscopy. Prog. Org. Coat. **46**, 273–279 (2003)
9. V.B. Miskovic-Stankovic et al., Corrosion behaviour of epoxy coatings on modified aluminium surfaces. Bull. Electrochem. **18**(8), 343–348 (2002)
10. V.B. Mišković-stanković, D.M. Dražić, M.J. Teodorović, Electrolyte penetration through epoxy coatings electrodeposited on steel. Corros. Sci. **37**(2), 241–252 (1995)

11. V.B. Mišković-Stanković, M.R. Stanić, D.M. Dražić, Corrosion protection of aluminium by a cataphoretic epoxy coating. Prog. Org. Coat. **36**(1), 53–63 (1999)
12. J.M. McIntyre, H.Q. Pham, Electrochemical impedance spectroscopy; a tool for organic coatings optimizations. Prog. Org. Coat. **27**(1–4), 201–207 (1996)
13. F. Mansfeld, Models for the impedance behavior of protective coatings and cases of localized corrosion. Electrochim. Acta. **38**(14), 1891–1897 (1993)
14. I.M. Zin et al., The mode of action of chromate inhibitor in epoxy primer on galvanized steel. Prog. Org. Coat. **33**(3–4), 203–210 (1998)
15. M. Musiani et al., Constant-phase-element behavior caused by coupled resistivity and permittivity distributions in films. J. Electrochem. Soc. **158**(12), C424–C428 (2011)
16. B. Hirschorn et al., Constant-phase-element behavior caused by resistivity distributions in films: II Applications. J. Electrochem. Soc. **157**(12), C452–C457 (2010)
17. B. Hirschorn et al., Constant-phase-element behavior caused by resistivity distributions in films: I. theory. J. Electrochem. Soc. **157**(12), C458–C463 (2010)
18. S. Amand et al., Constant-phase-element behavior caused by inhomogeneous water uptake in anti-corrosion coatings. Electrochim. Acta. **87**, 693–700 (2013)
19. F. Mansfeld, M.W. Kendig, S. Tsai, Evaluation of corrosion behavior of coated metals with AC impedance measurements. Corrosion **38**(9), 478–485 (1982)
20. M. Tomkiewicz, B. Aurian-Blajeni, Impedance of composite materials. J. Electrochem. Soc. **135**(11), 2743–2747 (1988)
21. A. Perrotta et al., Analysis of nanoporosity in moisture permeation barrier layers by electrochemical impedance spectroscopy. ACS Appl. Mater. Interfaces **7**(29), 15968–15977 (2015)
22. C.H. Hsu, F. Mansfeld, Concernng the conversion of the constant phase element parameter Y 0 into a capacitance. Corrosion **57**(9), 747–748 (2001)
23. N.K. Mehta, M.N. Bogere, Environmental studies of smart/self-healing coating system for steel. Prog. Org. Coat. **64**(4), 419–428 (2009)
24. S.J. Garcia et al., Self-healing anticorrosive organic coating based on an encapsulated water reactive silyl ester: synthesis and proof of concept. Prog. Org. Coat. **70**(2–3), 142–149 (2011)
25. S.J. Garcia, X. Wu, S. Van Der Zwaag, A combined electrochemical impedance spectroscopy and x-ray-computed tomography study of the effect of a silyl ester on delamination and underfilm pit formation in a coated AA7050 sample. Corrosion **70**(5), 475–482 (2014)
26. T. Breugelmans et al., Odd random phase multisine electrochemical impedance spectroscopy to quantify a non-stationary behaviour: theory and validation by calculating an instantaneous impedance value. Electrochim. Acta. **76**, 375–382 (2012)
27. Y. Van Ingelgem et al., Advantages of odd random phase multisine electrochemical impedance measurements. Electroanalysis **21**(6), 730–739 (2009)
28. B.A. Boukamp, Linear Kronig-Kramers transform test for immittance data validation. J. Electrochem. Soc. **142**(6), 1885–1894 (1995)
29. B.A. Boukamp, Practical application of the Kramers-Kronig transformation on impedance measurements in solid state electrochemistry. Solid State Ionics **62**(1–2), 131–141 (1993)
30. J.B. Jorcin et al., Investigation of the self-healing properties of shape memory polyurethane coatings with the 'odd random phase multisine' electrochemical impedance spectroscopy. Electrochim. Acta. **55**(21), 6195–6203 (2010)
31. T. Breugelmans et al., Odd random phase multisine EIS for organic coating analysis. Prog. Org. Coat. **69**(2), 215–218 (2010)
32. J.B. Jorcin et al., Delaminated areas beneath organic coating: a local electrochemical impedance approach. Corros. Sci. **48**(7), 1779–1790 (2006)
33. P.L. Bonora, F. Deflorian, L. Fedrizzi, Electrochemical impedance spectroscopy as a tool for investigating underpaint corrosion. Electrochim. Acta. **41**(7–8), 1073–1082 (1996)
34. M. AbdolahZadeh, S. van der Zwaag, S.J. Garcia, Assessment of healed scratches in intrinsic healing coatings by AC/DC/AC accelerated electrochemical procedure. J. Coat. Sci. Technol. (2015) accepted

35. S.J. García et al., Evaluation of cure temperature effects in cataphoretic automotive primers by electrochemical techniques. Prog. Org. Coat. **60**(4), 303–311 (2007)
36. S.J. Garcia, J. Suay, Application of electrochemical techniques to study the effect on the anticorrosive properties of the addition of ytterbiurn and erbium triflates as catalysts on a powder epoxy network. Prog. Org. Coat. **57**(3), 273–281 (2006)
37. S.J. García, J. Suay, A comparative study between the results of different electrochemical techniques (EIS and AC/DC/AC): application to the optimisation of the cataphoretic and curing parameters of a primer for the automotive industry. Prog. Org. Coat. **59**(3), 251–258 (2007)
38. S.J. García, J. Suay, Optimization of deposition voltage of cataphoretic automotive primers assessed by EIS and AC/DC/AC. Prog. Org. Coat. **66**(3), 306–313 (2009)
39. T.A. Markley, M. Forsyth, A.E. Hughes, Corrosion protection of AA2024-T3 using rare earth diphenyl phosphates. Electrochim. Acta **52**(12), 4024–4031 (2007)
40. D. Ho et al., Cerium dibutylphosphate as a corrosion inhibitor for AA2024-T3 aluminum alloys. J. Electrochem. Soc. **153**(9), B392–B401 (2006)
41. S.J. Garcia et al., The influence of pH on corrosion inhibitor selection for 2024-T3 aluminium alloy assessed by high-throughput multielectrode and potentiodynamic testing. Electrochim. Acta. **55**(7), 2457–2465 (2010)
42. Y.J. Tan, An experimental comparison of three wire beam electrode based methods for determining corrosion rates and patterns. Corros. Sci. **47**(7), 1653–1665 (2005)
43. Y.J. Tan, S. Bailey, B. Kinsella, Mapping non-uniform corrosion using the wire beam electrode method. II. Crevice corrosion and crevice corrosion exemption. Corros. Sci. **43**(10), 1919–1929 (2001)
44. Y.J. Tan et al., Mapping corrosion kinetics using the wire beam electrode in conjunction with electrochemical noise resistance measurements. J. Electrochem. Soc. **147**(2), 530–539 (2000)
45. S.R. Taylor, B.D. Chambers, in *Proceedings of the 4th International Symposium on Aluminium Surface Science and Technology, Beaune, France*, May (2006), Proceedings to be published in: ATB Metallurgie, 45 (1–4) (2006) 418. 2006
46. B.D. Chambers, S.R. Taylor, M.W. Kendig, Rapid discovery of corrosion inhibitors and synergistic combinations using high-throughput screening methods. Corrosion **61**(5), 480–489 (2005)
47. T.H. Muster et al., A rapid screening multi-electrode method for the evaluation of corrosion inhibitors. Electrochim. Acta. **54**(12), 3402–3411 (2009)
48. S.J. García, J.M.C. Mol, T.H. Muster, A.E. Hughes, J. Mardel, T. Miller, T. Markely, H. Terryn, J.H.W. de Wit, in *Green Inhibitors*, ed. by L. Fedrizzi. Advances in the Selection and use of Rare-Earth-Based Inhibitors for Self Healing Organic Coatings, Accepted for publication in Self-Healing Properties of New Surface Treatments. (EFC-Maney Publishing, 2011)
49. T.H. Muster et al., A review of high throughput and combinatorial electrochemistry. Electrochim. Acta. **56**(27), 9679–9699 (2011)
50. S.J. Garcia et al., Validation of a fast scanning technique for corrosion inhibitor selection: influence of cross-contamination on AA2024-T3. Surf. Interface Anal. **42**(4), 205–210 (2010)
51. B.D. Chambers, S.R. Taylor, The high throughput assessment of aluminium alloy corrosion using fluorometric methods. Part II - A combinatorial study of corrosion inhibitors and synergistic combinations. Corros. Sci. **49**(3), 1597–1609 (2007)
52. B.D. Chambers, S.R. Taylor, High-throughput assessment of inhibitor synergies on aluminum alloy 2024-T3 through measurement of surface copper enrichment. Corrosion **63**(3), 268–276 (2007)
53. P.A. White et al., High-throughput channel arrays for inhibitor testing: proof of concept for AA2024-T3. Corros. Sci. **51**(10), 2279–2290 (2009)
54. P.A. White et al., A new high-throughput method for corrosion testing. Corros. Sci. **58**, 327–331 (2012)

55. H. Böhni, T. Suter, F. Assi, Micro-electrochemical techniques for studies of localized processes on metal surfaces in the nanometer range. Surf. Coat. Technol. **130**(1), 80–86 (2000)
56. T. Suter, H. Böhni, Microelectrodes for studies of localized corrosion processes. Electrochim. Acta. **43**(19–20), 2843–2849 (1998)
57. M.M. Lohrengel, A. Moehring, M. Pilaski, Capillary-based droplet cells: limits and new aspects. Electrochim. Acta. **47**(1), 137–141 (2001)
58. T. Suter, R.C. Alkire, Microelectrochemical studies of pit initiation at single inclusions in Al 2024-T3. J. Electrochem. Soc. **148**(1), B36–B42 (2001)
59. F. Andreatta, H. Terryn, J.H.W. De Wit, Corrosion behaviour of different tempers of AA7075 aluminium alloy. Electrochim. Acta. **49**(17–18), 2851–2862 (2004)
60. F. Andreatta, H. Terryn, J.H.W. de Wit, Effect of solution heat treatment on galvanic coupling between intermetallics and matrix in AA7075-T6. Corros. Sci. **45**(8), 1733–1746 (2003)
61. J.O. Park, T. Suter, H. Böhni, Role of manganese sulfide inclusions on pit initiation of super austenitic stainless steels. Corrosion **59**(1), 59–67 (2003)
62. T. Suter, H. Böhni, A new microelectrochemical method to study pit initiation on stainless steels. Electrochim. Acta. **42**(20–22), 3275–3280 (1997)
63. V.S. Rao, H.S. Kwon, Corrosion Studies of Fe3Al – Fe3AlC intermetallics in 0.25 N H2SO4 using microelectrochemical method and SAES analysis. J. Electrochem. Soc. **154**(5), C255–C260 (2007)
64. N. Birbilis et al., Inhibition of AA2024-T3 on a phase-by-phase basis using an environmentally benign inhibitor, cerium dibutyl phosphate. Electrochem. Solid State Lett. **8**(11), C180–C183 (2005)
65. F. Andreatta et al., Localized corrosion inhibition by cerium species on clad AA2024 aluminium alloy investigated by means of electrochemical micro-cell. Corros. Sci. **65**, 376–386 (2012)
66. I. Recloux, Y. Gonzalez-Garcia, M-E. Druart, K. Khelifa, Ph. Dubois, J.M.C. Mol, M-G. Olivier, Active and passive protection of AA2024-T3 by an hybrid inhibitor doped mesoporous sol-gel and top coating system. Prog. Org. Coat. (2015) submitted
67. H.S. Isaacs, The measurement of the galvanic corrosion of soldered copper using the scanning vibrating electrode technique. Corros. Sci. **28**(6), 547–558 (1988)
68. H.S. Isaacs, G. Kissel, Surface preparation and pit propagation in stainless steels. J. Electrochem. Soc. **119**(12), 1628–1632 (1972)
69. F. Zou et al., in *Materials Science Forum*. Application of Scanning Vibrating Electrode Techniques to Study the Degradation of Coil-Coated Steel at Edges (1998), p. 83–92
70. H.S. Isaacs, Use of the scanning vibrating electrode technique for detecting defects in ion vapor-deposited aluminum on steel. Corrosion **43**(10), 594–598 (1987)
71. R.M. Souto et al., Investigating corrosion processes in the micrometric range: a SVET study of the galvanic corrosion of zinc coupled with iron. Corros. Sci. **49**(12), 4568–4580 (2007)
72. M.J. Franklin, D.C. White, H.S. Isaacs, A study of carbon steel corrosion inhibition by phosphate ions and by an organic buffer using a scanning vibrating electrode. Corros. Sci. **33**(2), 251–260 (1992)
73. A.C. Bastos, M.G. Ferreira, A.M. Simões, Corrosion inhibition by chromate and phosphate extracts for iron substrates studied by EIS and SVET. Corros. Sci. **48**(6), 1500–1512 (2006)
74. S. Kallip et al., A multi-electrode cell for high-throughput SVET screening of corrosion inhibitors. Corros. Sci. **52**(9), 3146–3149 (2010)
75. S. Kallip et al., Synergistic corrosion inhibition on galvanically coupled metallic materials. Electrochem. Commun. **20**(1), 101–104 (2012)
76. S.V. Lamaka et al., Nanoporous titania interlayer as reservoir of corrosion inhibitors for coatings with self-healing ability. Prog. Org. Coat. **58**(2–3), 127–135 (2007)
77. D. Raps et al., Electrochemical study of inhibitor-containing organic-inorganic hybrid coatings on AA2024. Corros. Sci. **51**(5), 1012–1021 (2009)

78. M.L. Zheludkevich, J. Tedim, M.G.S. Ferreira, "Smart" coatings for active corrosion protection based on multi-functional micro and nanocontainers. Electrochim. Acta. **82**, 314–323 (2012)
79. M.L. Zheludkevich et al., On the application of electrochemical impedance spectroscopy to study the self-healing properties of protective coatings. Electrochem. Commun. **9**(10), 2622–2628 (2007)
80. M. Marenzana et al., Bone as an ion exchange organ: evidence for instantaneous cell-dependent calcium efflux from bone not due to resorption. Bone **37**(4), 545–554 (2005)
81. J.G. Kunkel et al., in *Plant Electrophysiology: theory and Methods.* Use of Non-Invasive Ion-Selective Microelectrode Techniques for the Study of Plant Development (2006), p. 109–137
82. L. Shabala et al., Non-invasive microelectrode ion flux measurements to study adaptive responses of microorganisms to the environment. FEMS Microbiol. Rev. **30**(3), 472–486 (2006)
83. C.E.M. Berger, B.R. Horrocks, H.K. Datta, Application of ion-selective microelectrodes to the detection of calcium release during bone resorption. Electrochim. Acta. **44**(16), 2677–2683 (1999)
84. S.V. Lamaka et al., Monitoring local spatial distribution of Mg2+, pH and ionic currents. Electrochem. Commun. **10**(2), 259–262 (2008)
85. F. Sundfors et al., Microcavity based solid-contact ion-selective microelectrodes. Electroanalysis **18**(13–14), 1372–1378 (2006)
86. R.E. Gyurcsányi et al., Novel polypyrrole based all-solid-state potassium-selective microelectrodes. Analyst **123**(6), 1339–1344 (1998)
87. G. Gyetvai et al., Solid contact micropipette ion selective electrode for potentiometric SECM. Electroanalysis **19**(10), 1116–1122 (2007)
88. M.G. Taryba, S.V. Lamaka, Plasticizer-free solid-contact pH-selective microelectrode for visualization of local corrosion. J. Electroanal. Chem. **725**, 32–38 (2014)
89. E.A. Zdrachek et al., H+-selective microelectrodes with optimized measuring range for corrosion studies. Sens. Actuat. B: Chem. **207**(PB), 967–975 (2015)
90. P. Bühlmann, E. Pretsch, E. Bakker, Carrier-based ion-selective electrodes and bulk optodes. 2. Ionophores for potentiometric and optical sensors. Chem. Rev. **98**(4), 1593–1687 (1998)
91. J. Bobacka, A. Ivaska, A. Lewenstam, Potentiometric ion sensors. Chem. Rev. **108**(2), 329–351 (2008)
92. A.C. Bastos et al., Localised measurements of pH and dissolved oxygen as complements to SVET in the investigation of corrosion at defects in coated aluminum alloy. Electroanalysis **22**(17–18), 2009–2016 (2010)
93. M. Taryba et al., The combined use of scanning vibrating electrode technique and micro-potentiometry to assess the self-repair processes in defects on "smart" coatings applied to galvanized steel. Electrochim. Acta. **56**(12), 4475–4488 (2011)
94. O.V. Karavai et al., Localized electrochemical study of corrosion inhibition in microdefects on coated AZ31 magnesium alloy. Electrochim. Acta. **55**(19), 5401–5406 (2010)
95. A.J. Bard et al., Scanning electrochemical microscopy. Introduction and principles. Anal. Chem. **61**(2), 132–138 (1989)
96. A.J. Bard, M.V. Mirkin (ed.), *Scanning Electron Microscopy* (Marcel-Dekker, New York, 2001)
97. L. Niu et al., Application of scanning electrochemical microscope in the study of corrosion of metals. J. Mater. Sci. **44**(17), 4511–4521 (2009)
98. K. Mansikkamäki et al., Adsorption of benzotriazole on the surface of copper alloys studied by SECM and XPS. J. Electrochem. Soc. **153**(8), B311–B318 (2006)
99. J. Izquierdo et al., Scanning microelectrochemical characterization of the anti-corrosion performance of inhibitor films formed by 2-mercaptobenzimidazole on copper. Prog. Org. Coat. **74**(3), 526–533 (2012)

100. A.C. Bastos et al., Imaging concentration profiles of redox-active species in open-circuit corrosion processes with the scanning electrochemical microscope. Electrochem. Commun. **6** (11), 1212–1215 (2004)
101. A.M. Simoes et al., SVET and SECM imaging of cathodic protection of aluminium by a Mg-rich coating. Corros. Sci. **49**(10), 3838–3849 (2007)
102. A.C. Bastos et al., Application of the scanning electrochemical microscope to the examination of organic coatings on metallic substrates. Prog. Org. Coat. **53**(3), 177–182 (2005)
103. R.M. Souto et al., On the use of mercury-coated tips in scanning electrochemical microscopy to investigate galvanic corrosion processes involving zinc and iron. Corros. Sci. **55**, 401–406 (2012)
104. Y. González-García et al., SECM study of defect repair in self-healing polymer coatings on metals. Electrochem. Commun. **13**(2), 169–173 (2011)
105. Y. Gonzalez-Garcia et al., A combined redox-competition and negative-feedback SECM study of self-healing anticorrosive coatings. Electrochem. Commun. **13**(10), 1094–1097 (2011)
106. A. Pilbáth et al., SECM study of steel corrosion under scratched microencapsulated epoxy resin. Prog. Org. Coat. **75**(4), 480–485 (2012)
107. L.C. Abodi et al., Modeling localized aluminum alloy corrosion in chloride solutions under non-equilibrium conditions: steps toward understanding pitting initiation. Electrochim. Acta. **63**, 169–178 (2012)
108. M.G. Taryba et al., Novel use of a micro-optode in overcoming the negative influence of the amperometric micro-probe on localized corrosion measurements. Corros. Sci. **95**, 1–5 (2015)
109. R.S. Lillard, P.J. Moran, H.S. Isaacs, Novel method for generating quantitative local electrochemical impedance spectroscopy. J. Electrochem. Soc. **139**(4), 1007–1012 (1992)
110. V.M. Huang et al., Local electrochemical impedance spectroscopy: a review and some recent developments. Electrochim. Acta. **56**(23), 8048–8057 (2011)
111. R.M. Souto et al., in *ECS Transactions. Local Electrochemical Impedance Spectroscopy Investigation of Corrosion Inhibitor Films on Copper* (2012)
112. D. Snihirova, S.V. Lamaka, M.F. Montemor, "SMART" protective ability of water based epoxy coatings loaded with CaCO 3 microbeads impregnated with corrosion inhibitors applied on AA2024 substrates. Electrochim. Acta. **83**, 439–447 (2012)
113. D. Snihirova, S.V. Lamaka, M. Taryba, A.M. Salak, S. Kallip, M.L. Zheludkevich, M.G.S. Ferreira, M.F. Montemor, Hydroxyapatite microparticles as feedback-active reservoirs of corrosion inhibitors. ACS Appl. Mater. Interfaces **2**(11), 3011–3022 (2010)